THE JOURNAL OF PHYSICAL CHEMISTRY B

Article

pubs.acs.org/JPCB

Budding Behavior of Multi-Component Vesicles

Jianfeng Li,* Hongdong Zhang,* and Feng Qiu

The State Key Laboratory of Molecular Engineering of Polymers, Department of Macromolecular Science, Fudan University, Shanghai 200433, China

ABSTRACT: For multicomponent vesicles, the line tension of domain boundaries and the component-dependent elastic properties (e.g., spontaneous curvatures) are the two most important factors that mediate the budding behaviors of these vesicles. This paper especially focuses on their effects on the budding types and the budding number of a two-component vesicle. We found that the budding number is mainly determined by the component-dependent elastic properties while the budding types mediated by line tensions. A phase diagram is also obtained showing three different types of phase regions: (i) partially budding, (ii) partially bud-off, and (iii) totally bud-off regions. These inspiring results are, however, derived from a very simple spherical-cap model, and have been tested by computer simulations showing good agreement. We emphasize that, besides testing the spherical-cap model, the computer simulation techniques developed in the current work can be easily extended to other systems involving multicomponent vesicles.

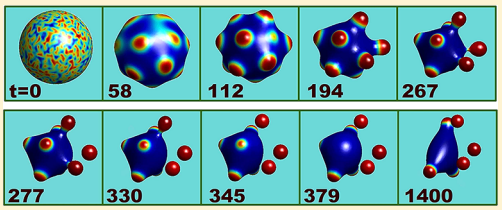

INTRODUCTION

Multicomponent membranes[1] consist of more than one species of lipid molecules. In the last two decades, such membranes have been extensively studied both experimentally[2−5] and theoretically[6−19] due to the following two reasons. First, biomembranes are multicomponent membranes.[20] Second, multicomponent vesicles exhibit some amazing physical properties that have not been observed for single-component vesicles.[21,22] In particular, such a vesicle can form intramembrane domains and undergo domain-induced budding, usually with many buds including partially budding buds as well as some bud-off buds.

In theory, the budding behaviors of two-component vesicles or membranes have been previously studied from both dynamical[7,9−13] and equilibrium[6,8,14−18] perspectives. For budding dynamics,[7,9−13] various simulation techniques have been developed to obtain the scaling laws of kinetics. Vesicles with many buds have also been observed in these simulations. For instance, Kohyama et al.[10] have employed a dynamic triangulation model combining with a Monte Carlo simulation to study the role of line tension and spontaneous curvature for the budding of crystalline domains in fluid vesicles. However, dynamical simulations alone cannot determine whether a many-bud state is a stable state or just a trapped, metastable state, since in a flat two-dimensional system two immiscible components will finally separate into two macrodomains.

Therefore, in recent years, the equilibrium properties of multicomponent vesicles have begun to regain the interest of theorists.[14−18] In the early days, equilibrium properties of such vesicles were analytically studied for two special cases, 1-D membranes[15] (embedded in a 2D plane) and membranes with rotational symmetry.[14,15] Recently, several interesting works[16−18] have been devoted to understanding the influence of the component-dependent elastic properties on the budding behavior of multicomponent vesicles. In particular, Gutlederer et al.[16] and Hu et al.[18] extensively studied the partially budding behavior of a multicomponent vesicle under various conditions and obtained fruitful and inspiring results. By comparing the energies of different metastable states, they found that a many-bud state aforementioned can be stable within a wide range of parameter settings. On the other hand, partially budding buds, bud-off buds, and other morphologies (or budding types) have been studied using a coarse grained model together with a continuum-model analysis by Zheng et al.[17] and they observed many interesting vesicle shapes like biconcave, starfish, and capsules. Those works basically arrive at the same conclusion that the line tension of domain boundaries is the main driving force for budding,[14] while the component-property difference will further complicate the final budding configurations.[15−18] However, the relationship between the component-dependent properties and the budding behavior still remains somehow elusive. In particular, we are still not clear about how the component-dependent properties determine the number of buds especially for vesicles with no symmetries imposed. The reasons for this are largely because former axisymmetrical assumptions[14,15] are not applicable here and, at the same time, the above simulations[16−18] still have difficulties in finding all stable states of different budding types for such vesicles.

In contrast, Lipowsky[6] suggested a very simple spherical-cap model to study the budding behavior of two-component planar membranes. The spherical-cap model is simple but found to be effective in addressing the basic physics regarding the involved budding process. Therefore, in this article, we shall study the equilibrium properties of a two-component vesicle using the same simple model but for closed vesicles, focusing on the influences of domain line tension and component-dependent

Received: August 13, 2012
Revised: October 17, 2012
Published: November 26, 2012

   dx.doi.org/10.1021/jp308043y | J. Phys. Chem. B 2013, 117, 843−849

elastic properties. Different components may have different elastic properties such as bending rigidities, Gaussian moduli, and spontaneous curvatures. Here, we only consider the effects of the spontaneous curvature difference, leaving other possibilities to the future publications. This simple spherical-cap model enables us to calculate the global minimum-energy states very easily and accurately. By this model, a phase diagram is constructed and exhibits three different types of phase regions: (i) partially budding, (ii) partially bud-off, and (iii) totally bud-off regions. The (i) phase regions have been studied by refs 15, 16, and 18, while (ii) phase regions have been especially discussed in ref 17. (iii) phase regions are new, and the knowledge of these regions is valuable, since many biological phenomena involve bud-off processes.[20] However, this model (though with no axisymmetrical assumption) is still oversimplified and needs to be tested. Therefore, a computer simulation based on a dynamical-triangulation method[23] and dissipative dynamics[7] will be further developed to support the above findings.

METHODOLOGIES

A Spherical-Cap Model for Multi-Component Vesicles. In the spherical-cap model[6] for two-component vesicles, we assume that the two membrane lipids A and B have already separated into the pure A and pure B domains. A and B membrane patches share the same bending rigidity, κ, and are both with vanishing Gaussian bending energy, while their preferred curvatures or spontaneous curvatures, C_A and C_B, may differ from each other. In most cases, it is reasonable to assume that the dominant component B has zero spontaneous curvature and the left component tends to bud out, i.e., $C_B = 0$ and $C_A > 0$.[16,17] As illustrated in Figure 1, the final morphology of the two-component vesicle is assumed to be with n_p spherical caps (partially budding buds) and n_t spheres (bud-off buds) both composed of pure A components; and n_p spherical caps are adjacent to the original, B-component sphere with n_p holes in it. By the above setting, the energy of such a vesicle can be expressed in terms of

$$F = \sum_{1}^{n_t} 4\pi {R_i}^2 f_{i,A} + \sum_{1}^{n_p} 2\pi {R_k}^2 (1 + \cos\theta_k) f_{k,A} + (4\pi {R_s}^2 - \sum_{1}^{n_p} \pi {R_k}^2 \sin^2\theta_k) f_{s,B} + \gamma \sum_{1}^{n_p} 2\pi R_k \sin\theta_k \quad (1)$$

where $f_{i(k),A(B)}$ are bending energy densities $\kappa(2/R_{i(k)} - C_{A(B)})^2/2$ with R_i, R_k, amd R_s being the radii of bud-off spheres, budding caps, and B-component sphere, respectively. γ is the line tension of the A/B domain boundaries. For the present model, we did not include osmotic pressure and the vesicle volume is, therefore, freely adapting; this assumption has also been employed in several previous theoretical works[7,9,17] involving multicomponent vesicles. However, the total membrane area, $4\pi {R_0}^2$, is fixed using the following constraints: $[4\pi {R_s}^2 - \sum_1^{n_p} \pi {R_k}^2 \sin^2\theta_k] = 4\pi {R_0}^2(1 - \bar{\phi}_A)$ and $\sum_1^{n_t} 4\pi {R_i}^2 + \sum_1^{n_p} 2\pi {R_k}^2(1 + \cos\theta_k] = 4\pi {R_0}^2 \bar{\phi}_A$, where $\bar{\phi}_A$ is the overall volume fraction of the A component. Because near the critical composition the A component usually forms belt-like domains for small C_A, which obviously cannot be described by the spherical-cap model, we only study the off-critical case and set $\bar{\phi}_A = 0.35$ throughout this work.

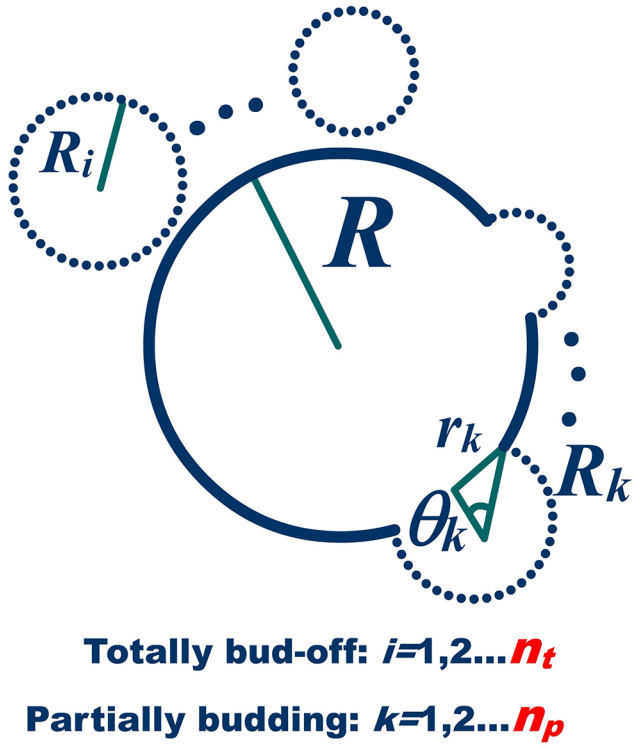

Figure 1. Schematic illustration of the spherical-cap model (SCM) for two-component vesicles. The "$n_p + n_t$" notations (e.g., "2 + 1") are used to denote the final vesicle configuration, with n_p and n_t being the number of the partially budding and bud-off buds, respectively (see also Figure 2). A-component domains are denoted by dotted arcs while B-component with solid ones.

Apparently, the final vesicle configuration of the spherical-cap model described above is determined by the two controlled parameters: the reduced line tension $R_0\gamma/\kappa$ and the reduced spontaneous curvature R_0C_A. The equilibrium stable configuration for a fixed $(R_0\gamma/\kappa, C_AR_0)$ can be obtained via the optimizations of eq 1 with respect to the numbers, sizes, and budding angles of buds, i.e., n_t, n_p, R_i, R_k, R_s, and θ_k. To ensure what we obtain is really the global minimum, we enumerate nearly all possible values of these parameters with the only one constraint that $n_t + n_p \leq 7$ and compare the corresponding energies obtained from eq 1 to determine the global minimum state.

Simulation Method for Multi-Component Vesicles. The spherical-cap model described above will be checked by a dissipative dynamical simulation in the Results section. The simulation method closely follows Taniguchi's work,[7] where he used a deformable but a network topology fixed triangulation together with a diffusive dynamics to describe the deformation of a two-component vesicle. In the present work, to further account for the large deformation of the vesicle, we have incorporated into the current method the dynamical triangulation techniques.[9,10,23] In a recent work,[24] we have successfully applied these techniques to simulate the large deformations of the gold nanostructures observed in the experiments.

To describe the diffusive dynamics, the order parameter of components $\phi = \phi_A - \phi_B$ is introduced. In terms of this parameter, the free energy of the A/B vesicle can be expressed as $F = F_1 + F_2$

$$F_1 = \frac{\kappa}{2}\int (H - C_A\phi_A)^2 \, dA + \lambda S \quad (2)$$

dx.doi.org/10.1021/jp308043y | J. Phys. Chem. B 2013, 117, 843−849

$$F_2 = \int \left[\frac{b}{2}(\nabla\phi)^2 - \frac{a_2}{2}\phi^2 + \frac{a_4}{4}\phi^4 \right] dA \quad (3)$$

where F_1 is the shape energy with $H/2$ being the mean curvature and λ the Lagrange multiplier to constrain the total area of the vesicle. F_2 is the Ginzburg–Landau free energy where $\sqrt{b}$ is a correlation length and a_2 and a_4 are two phenomenological parameters. These three parameters are all set to 1 and closely related to the domain line tension by the relation $\gamma \approx 2(2ba_2)^{1/2}/3$.[25] In the Results section, we study the effect of the reduced line tension $\gamma R_0/\kappa$ by tuning the bending modulus κ (see Figure 5) other than by varying the phenomenological parameters. With the above energetic expressions (eqs 2 and 3), the budding process of two-component vesicles can be properly described by the dissipative dynamics[7]

$$\frac{\partial \mathbf{r}}{\partial t} = L_r \frac{\delta F}{\delta \mathbf{r}} \quad (4)$$

and

$$\frac{\partial \phi}{\partial t} = L_\phi \nabla^2 \frac{\delta F}{\delta \phi} \quad (5)$$

where $\mathbf{r}$ represents the vesicle shape and L_r and L_ϕ are two kinetic coefficients, which are set to 1/8 and 1, respectively. The integration of these two kinetic equations was performed using the Euler scheme, where Δt is set to 0.001. The radius of the initial vesicle is $R_0 = 12$ with 2562 vertices in the triangulation mesh. It should be noted that, in order to be compatible with the dynamical triangulation, we only constrain the total area other than the local area. In addition, the thermal fluctuations are not included in the current study.

In Taniguchi's work,[7] the above dynamical equations are employed to study the dynamical behaviors of the vesicle deformation coupling with the phase separations. In the current work, we shall focus on the equilibrium behavior and these equations are used to minimize the system energy instead: if the dynamics is evolved for a sufficiently long time, the obtained vesicle shape should correspond to a local minimum state (see the Results section).

Herein, we especially discuss the dynamical triangulation method, which is an important technique for simulating large deformations of membranes based on the traditional continuum membrane theory. The dynamical triangulation method of the current study is mostly based on a free software Surface Evolver,[23] but we have made important improvements about this method and the corresponding simulation codes are entirely composed by ourselves. Specifically, the improved method consists of several surface operations:

(i) Equiangulation. The basic idea of this surface operation is to eliminate the obtuse triangles by flipping edges (or bonds). A detailed description of this operation can be read in ref 23.

(ii) Vertex Averaging. As the dynamical process continues, the triangulated mesh may become not evenly woven or, in other words, the vertexes are not evenly distributed on the surface anymore. This uneven mesh will severely impair the numerical stability of the simulation. For the compensation, we redistribute the vertexes. The mesh is first refined and interpolated twice using the butterfly scheme,[26] and the number of the vertex will be increased by 16 times during this refinement. The A/B concentrations will also be interpolated and refined. Then, we "vertex-average" the original vertexes according to a method similar to that of ref 23 while we constrain the after-averaged positions on the refined mesh. The advantage of this promoted technique is that the repeating of the operation would not alter the shape of the membrane, while the vertex-averaging operation presented in ref 23 will actually change the shape after many times of the averaging, which will introduce "fake" dynamics into the budding process.

(iii) Removing Small Triangles or Edges. In some circumstances, we need to remove some small triangles or edges with areas or lengths much smaller (usually twice) than the averaged value.

(iv) Fission Process. This operation will be applied to a vesicle with an extremely small neck. When the neck size is smaller than some threshold, we try to cut the vesicle into two parts and let it evolve for some time to see whether the resulting state becomes more energetically favorable or not. If more favorable, we accept the fission process and continue the dynamics; if not, we go back to the before-fission state. Technically, the fission operation involves two steps: cutting the closed surface into two open surfaces with open edges and then closing these open surfaces by adding new vertexes and faces.

It should be noted that these operations have two sides: on the one hand, they can improve the numerical stability of the simulation dramatically and, on the other hand, some unexpected "fake" dynamics may be introduced into the simulation. To suppress the latter effect, we have first improved the surface operations of the Surface Evolver.[23] For example, the old version of "vertex averaging"[23] will change the shape of the surface and introduce fake dynamics, while the operation (ii) described above preserves the shape. Second, in our improved method, the computer program will automatically start these surface operations in between a couple of computer time steps but not very frequently, while, in the Surface Evolver,[23] the surface operations are started by hand. Third, since we only care about the equilibrium behavior of the system, whether the fission process described above really reflects the real dynamical situation does not concern us too much; nevertheless, we emphasize that this process can describe the real fission process properly if the energy barriers of the fission are available (e.g., obtained from other particle-based or field-based simulations[27]).

RESULTS

Phase Diagram by the Spherical-Cap Model. In this article, we especially study the influences of the domain line tension and the component-dependent spontaneous curvature on the budding behavior of two-component vesicles. Figure 2 shows the phase diagram of $(R_0\gamma/\kappa, C_A R_0)$ obtained by the spherical-cap model. It mainly involves three types of phase regions: (i) partially budding phase regions ($n_t = 0$) with all A domains only partially budding out when γ is small; (ii) partially bud-off phase regions ($n_p \neq 0$, $n_t \neq 0$) with some domains budding off the vesicle for median γ and nonzero C_A; and (iii) totally bud-off phase regions ($n_p = 0$) for big γ. The first two types of phase regions (i) and (ii) have been previously studied in refs 15–18, while the totally bud-off phase regions (iii) are new and have not been treated seriously before. Figure 2 actually presents the totally bud-off conditions for a two-component vesicle: when the A/B components have no preferred curvature difference, the critical line tension for the totally bud-off condition is $R_0\gamma/\kappa > 4.56$ (not shown); increasing this difference will lower this critical value a lot to about 0.73. However, you will be shown in the simulation

dx.doi.org/10.1021/jp308043y | J. Phys. Chem. B 2013, 117, 843–849

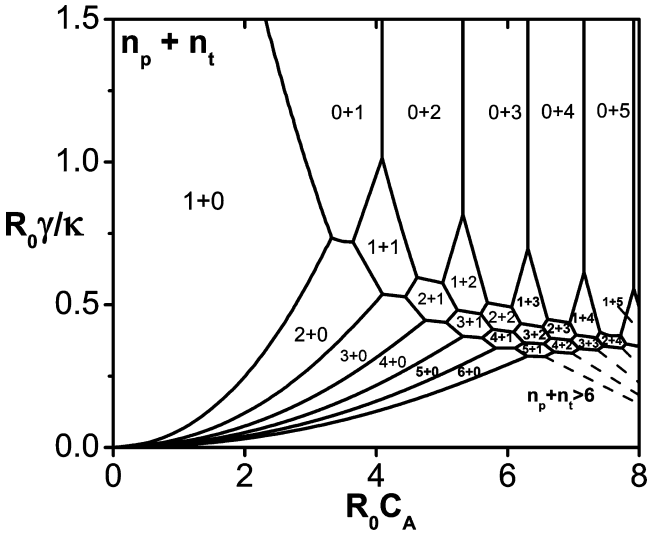

Figure 2. Phase diagram of (γ, C_A) obtained by the spherical-cap model at $\bar{\phi}_A = 0.35$. The "$n_p + n_t$" notations (e.g., "2 + 1") are used to denote the final vesicle configuration, with n_p and n_t being the number of the partially budding and bud-off buds, respectively (see also Figure 1).

section that kinetics will complicate these conditions further. The above bud-off conditions may be important for those biological processes involving bud-off vesicles such as the communications between the cell membranes and interior organelles.[20,22]

Two more noticeable features about the diagram's structures are that all (ii)-type phase regions together form a honeycomb structure, while the phase regions with the same total buds ($n_p + n_t$), as a whole, look like a crab's foot with its tip pointing at the origin of the diagram.

The spherical-cap model is simple, yet the physics contained in the phase diagram is rich and inspiring. From Figure 2, the line tension of domain boundaries is found to be the main driving force for budding. In particular, it determines the budding types of a two-component vesicle. This effect of the line tension has long been recognized and studied extensively both in theory[14,15] and experiment.[3]

However, the effects of the component-dependent elastic constants on the budding behavior receive less attention and, thus, still remain somehow elusive. In particular, how the budding number and budding type depend on these constants is still unclear for vesicles with no symmetries imposed. The phase diagram actually quantitatively shows this dependence. In particular, for big line tensions, we have

$$\sqrt{n_t + 1} + \sqrt{n_t} = \sqrt{\bar{\phi}_A}\, C_A R_0 \qquad (6)$$

which actually defines the phase boundaries of (iii)-type phase regions and can be obtained by minimizing eq 1 for $n_p = 0$. Overall, the spontaneous curvature difference between the A/B components will increase the number of buds. The reason for this is that, when $C_A = 0$, to lower the overall curvature of the budding domain, the "1 + 0" or "0 + 1" configuration with a bigger-size bud is obviously a better choice; when $C_A > 0$, A membrane patches need to match the preferred curvature, the vesicle configuration with more buds may be more favorable. A similar conclusion has also been obtained in ref 15, but their work is mainly restricted to the partially budding phase regions (i.e., $n_t = 0$). It is also important to note that (i) when the Gaussian modulus is present, the stability of a many-bud state compared to that of bud-off vesicles is mainly controlled by the Gaussian curvature;[8] (ii) many-bud budding behavior can also be observed in single-component vesicles,[21] but the driving forces for budding there are the area difference between the leaflets of bilayer and the fixed area−volume ratio constraint other than the domain line tension.

Phase Diagram by Dissipative Dynamics Simulations. The above spherical-cap model is obviously oversimplified. If it had not been tested by other methods or simulations, it would be suspected. Therefore, we have performed some numerical simulations based on a triangulation-mesh method similar to Taniguchi's work[7] to test the above analysis.

Figure 3 presents a typical time evolution picture of the budding dynamics of a two-component vesicle: an initially

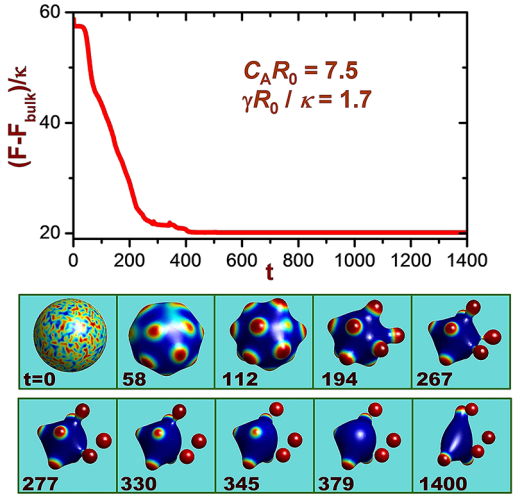

Figure 3. (upper panel) The energy profile of the dynamical evolution of a random-phase initial state into a "3 + 3" state with three bud-off buds at $\bar{\phi}_A = 0.35$, $R_0C_A = 7.5$, $\kappa = 6.67$, and $b = a_2 = a_4 = 1$. The effective reduced line tension is given by $\gamma R_0/\kappa \approx 2(2ba_2)^{1/2}R_0/3\kappa$. The bulk-phase energy $F_{bulk} = 4\pi R_0^2(-a_2\phi^2/2 + a_4\phi^4/4)|_{\phi=\pm1}$ has been excluded from the total membrane energy, since this energy only acts as a surface tension term which remains constant as the total area is conserved. (lower panel) The corresponding evolutionary snapshots at different computer time steps. The A-domains are shown in red while the B-domains in blue.

spherical vesicle gradually transforms into a "3 + 3"-type vesicle with three partially budding buds and three bud-off buds. It is exciting to find that we have successfully simulated the fission process using the triangulation-mesh method. It should be noted that we evolve the dynamics for a sufficiently long time, so the final states obtained here should, at least, correspond to the metastable states (see also the upper panel of Figure 3). However, the free energy landscape of the current system might have many local minima or metastable states for each parameter setting. Therefore, the above obtained "3 + 3" state might not be a global minimum. Actually, according to Figure 4, it is not ground stable (the ground stable state should be a "3 + 2"-type vesicle other than "3 + 3").

Nevertheless, the ground stable state can be determined by comparing the free energies of different metastable states evolved from different initial states. For example, Figure 4 employs 11 different initial states to determine the ground states at different reduced line tensions for $R_0C_A = 7.5$. For instance, it is clear that the configurations "0 + 4" will be

dx.doi.org/10.1021/jp308043y | J. Phys. Chem. B 2013, 117, 843−849

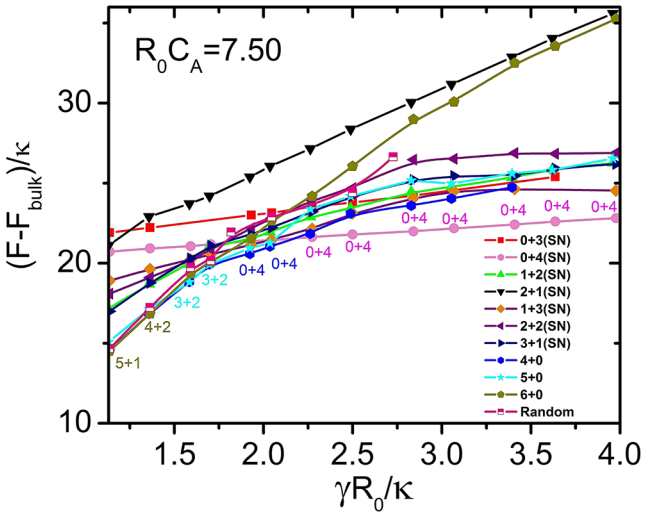

Figure 4. The energy profiles for 11 different initial states at $\bar{\phi}_A = 0.35$, $R_0C_A = 7.5$, and $b = a_2 = a_4 = 1$, where "1 + 2(SN)" indicates a two-component vesicle with one partially budding domain and two almost-bud-off domains but with a very *small neck* connecting to the mother vesicle. "Random" indicates the initial state is a spherical vesicle with the random phase. The final states of different initial states also depend on the reduced line tension; we label the ground stable configurations near the data points for each line tension. For the definition of $(F - F_{bulk})/\kappa$, please refer to the caption of Figure 3.

ground stable when $\gamma R_0/\kappa > 2.25$ according to the energy profiles in Figure 4. For different R_0C_A, different sets of initial states are required to determine the ground stable state for each parameter setting (e.g., only five initials are needed for R_0C_A = 4.0). By these ground stable states, the corresponding phase diagram of reduced spontaneous curvature R_0C_A and line tension $\gamma R_0/\kappa$ can be constructed.

Figure 5 shows such a phase diagram and the typical vesicle configurations for every phase region, which involves about 4000 × 24 h of computation on clusters. It should be first noted that the reduced line tension can be roughly expressed as $\gamma R_0/\kappa \approx 2(2ba_2)^{1/2}R_0/3\kappa$, which is actually tuned by varying the bending modulus κ for fixed b, a_2, and a_4. Just like the diagram by the spherical-cap model (SCM), there are three types of phase regions: (i) partially budding, (ii) partially bud-off, and (iii) totally bud-off phase regions. Every (i) and (iii) phase region in Figure 2 show up again in Figure 5; however, only some of the (ii)-type phase regions reappear in the current diagram. One possible reason may be that we only explore some discrete phase points in the phase space and the finer structures of the diagram require more calculations. In addition, the critical line tension for bud-off condition by the spherical-cap model is obviously much smaller than that of simulations. It might be because the spherical-cap model underestimates the energy barrier between the partially budding and bud-off states. Nevertheless, the present simulations qualitatively agree with the results of SCM. Furthermore, many of the vesicle configurations shown in Figure 5 can also be found in the experiments or other simulations. For example, configurations labeled with "1 + 0" with vanishing spontaneous curvature, "0 + 1", and "6 + 0" can be found in Baumgart et al.'s experiment,[3] while "2 + 0" and "3 + 0" have also been obtained by previous simulations by Gutlederer et al.[16] and Hu et al.[18] We have also reproduced some vesicle configurations observed in Zheng et al.'s work.[17] However, it should be noted that, in the experiment, the situation is much more complicated because

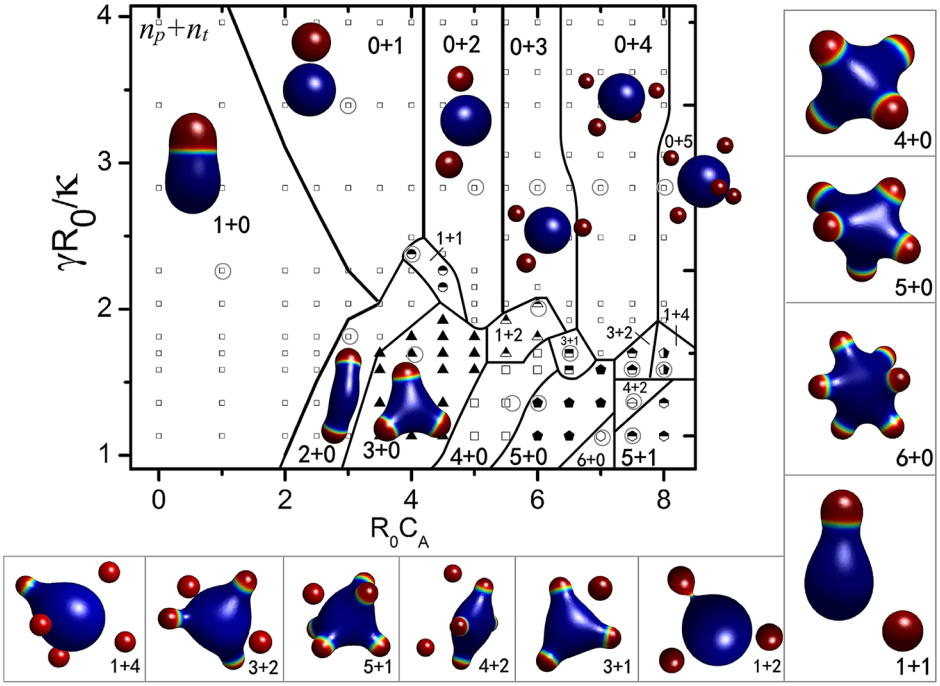

Figure 5. Phase diagram of $(\gamma R_0/\kappa, R_0C_A)$ obtained by the dynamical simulations at $\bar{\phi}_A = 0.35$ and $C_B = 0$. Note that the reduced line tension can be roughly expressed as $\gamma R_0/\kappa \approx 2(2ba_2)^{1/2}R_0/3\kappa$, which is actually tuned by varying the bending modulus κ for fixed b, a_2, and a_4. Because κ cannot be very big in simulations, unlike Figure 2, we cannot study the very small line tension region here. Various symbols like squares and solid triangles are used to indicate the calculated phase points. Except for the phase boundaries between "1 + 0" and "0 + 1" and "1 + 0" and "2 + 0", other phase boundaries are only drawn to guide the eye. The representative vesicle configurations for each phase region are also presented, which are calculated for the phase points labeled with gray circles.

dx.doi.org/10.1021/jp308043y | J. Phys. Chem. B 2013, 117, 843−849

the existence of the nonzero spontaneous curvature is not obvious and the membrane is actually composed of three components in this experiment.[3] Similarly, it is also difficult to make a quantitative comparison of our results to other simulation results mostly because the model parameters in different simulation models are usually defined in different ways; for example, Zheng et al.[17] model the membrane using a coarse grain model, while we employ the elastic continuum model based on the Helfrich[28] free energy, and it is difficult to make a quantitative (direct) comparison of the model parameters between these two models.

In experiments, the kinetics may further complicate the situation. For example, when $C_A R_0 = 8$ and $\gamma R_0/\kappa = 2.0$, a totally bud-off state "0 + 5" is the ground stable state (Figure 5); however, we found that a "4 + 3" configuration is obtained in a dynamical simulation started from a random-initial phase state, which should be most close to a real experimental situation, since most experiments start from random initial states. Therefore, the kinetics will further increase the number of domains or buds by trapping the vesicles in various metastable states. Accordingly, we find that it is indeed very hard to obtain the totally bud-off configurations with random initial states; most times, we end up with partially bud-off ones. In contrast, the totally bud-off regions dominate a large area of the phase space in Figure 5.

DISCUSSION

Budding behaviors of two-component vesicles have been studied by a simple spherical-cap model together with a series of dissipative dynamical simulations. By computing the phase diagrams at different spontaneous curvatures and domain line tensions, we have identified three major phase regions, i.e., partially budding, partially bud-off, and totally bud-off phase regions, respectively. In particular, partially budding phase regions have been extensively studied by Gutlederer et al.[16] and Hu et al.,[18] and partially bud-off phase regions with different topologies have been particularly investigated by Zheng et al.,[17] while the totally bud-off phase regions are new and have not been treated seriously before. Both the spherical-cap model and simulations show that the less dominant component can completely bud off the mother vesicle above some critical domain line tension (see Figures 2 and 5); increasing the spontaneous curvature can lower this critical value but will increase the number of bud-off buds at the same time (see eq 6). The above bud-off conditions may be important for those biological processes involving bud-off vesicles such as the communications between the cell membranes and interior organelles;[20,22] our calculations imply that, if a cell or vesicle wants to dump the unwanted lipid component, the spontaneous curvature of the unwanted component is important, which determines whether this component can be dumped completely as well as the size (also the number) of the dumping buds.

In our spherical-cap model, we assume that all the budding (bud-off) domains are with spherical-cap (spherical) shapes. This simple model setting enables us to calculate the global minimum-energy states easily and accurately. In fact, we can enumerate nearly all possible budding vesicle states at each parameter setting and compare the corresponding energies of these states to obtain the global minimum or ground stable states. Therefore, the phase diagram constructed from these states is accurate in this sense. In particular, this model gives the explicit expression (eq 6) for the phase boundaries between the totally bud-off phase regions in the phase diagram. Nevertheless, this model is oversimplified and not realistic, as the budding shapes observed in experiments are not ideally spherical; further, the model cannot consider the critical-composition case ($\bar{\phi}_A = \bar{\phi}_B = 0.5$), under which condition two components usually form bicontinuous phase domains and a spherical-cap assumption will not be valid anymore.

However, if the phase diagram can be verified by simulations, then it can still provide instructive and qualitative descriptions for the budding behavior of multicomponent vesicles. Therefore, we have also computed a phase diagram by a series of dissipative dynamical simulations showing qualitatively good agreements with that by the spherical-cap model. Our dissipative dynamical simulations are based on an elastic continuum model[7] (described by the Helfrich-type free energy[28]) for multicomponent vesicles, which employs a dynamical triangulation-mesh method together with diffusive dynamics for the phase separations of the two components. Previous simulations[16−18] for budding behavior of multicomponent vesicles are mostly based on the coarse-grained model which has been regarded as a better model than the elastic continuum model, mostly because previous simulations[7] based on the continuum model cannot describe the fission process. Our simulations have shown that the continuum model can also describe the fission process even though it cannot account for the molecular rearrangements[12] during the fission process. In addition, the simulations based on the continuum model have their own advantages. Because most previous theories[22] about vesicle deformations are based on continuum models, the simulations based on these models can be directly made compared with previous theories (though this work has not made such comparisons).

In addition to the above discussions, several comments can be made from the present work: (1) Most model assumptions of the current study (in both spherical-cap model and dissipative simulations) are the same as previous simulations[7,9,17,18] related to multicomponent vesicles. In particular, these calculations are all based on the spontaneous-curvature model. However, the physical origin of the spontaneous curvatures of different components is not very clear,[17] which might be due to the local compositional asymmetry between two leaflets of the bilayer. (2) In the present study, we only investigated the influences of the component-dependent spontaneous curvature on the budding behavior of multicomponent vesicles. However, many experiments show that the bending modulus is also a severely component-dependent parameter, and Gutlederer et al.[16] and Hu et al.[18] have carefully studied the influence of this dependence for the partially budding phase regions. It will be interesting to study how the component-dependent bending modulus affects the bud-off behavior of multicomponent vesicles in our future works. (3) In most previous works,[7,9,16−18] they have also considered the influence of different component compositions (i.e., $\bar{\phi}_A$), which is not accessible for the spherical-cap model due to the spherical-cap assumption; when $\bar{\phi}_A = 0.5$, the multicomponent vesicle may form "belt-like" A-domains. Nevertheless, just as other simulation methods, our simulation method can easily account for any component composition. (4) Our previous work[29] shows that microphase separations of A/B diblock copolymers can naturally form multiple domains on a rigid, closed spherical surface, where the chemical bonds linking the A/B blocks prevent A/B components from further separating into macro-phase domains. Similarly, current work indicates

that the presumable macro-phase separations on a deformable vesicle can also be inhibited under certain circumstances by the spontaneous-curvature bending energy, resulting in many-bud phases. This phenomenon has also been noticed by many other authors.[1,16−18] (5) Although in the current study, the simulations based on dynamical triangulations are employed only to test the results by the spherical-cap model, we emphasize that the results by these simulations themselves do reveal some important physics that have been neglected by the spherical-cap model. For instance, simulations show that the multicomponent vesicles might be easily trapped in the metastable states with more buds than in its stable state, while the spherical-cap model alone cannot address the mechanism behind these metastabilities properly. Furthermore, the simulation techniques developed in this work can be easily extended to other systems involving multicomponent vesicles, where the spherical-cap assumption might be no longer applicable (see also comment (3)). For example, when the area−volume ratio is big, the multicomponent vesicles form tubular shapes,[4] which are certainly not suitable to be depicted as spherical caps.

CONCLUSIONS

In summary, we study the budding behavior of a two-component vesicle by the spherical-cap model (SCM) together with computer simulations. We find that the component-dependent elastic properties will determine the number of buds and affect the budding types as well. In particular, the spontaneous curvature difference between the two components will increase the budding number. The phase diagrams by the SCM and the simulations are also obtained, both showing three different types of phase regions, i.e., partially budding, partially bud-off, and totally bud-off phase regions.

The current study only considered the component-dependent spontaneous curvature, and other component-dependent properties will be included in our future studies. To our best knowledge, we have first reported a simulation method based on the triangulated mesh and diffusive dynamics, that can properly describe large deformations and the fission process for multicomponent vesicles. In addition, we believe we have provided a general theoretical framework for the study of multicomponent vesicles.

AUTHOR INFORMATION

Corresponding Author

*E-mail: lijf@fudan.edu.cn (J.L.); zhanghd@fudan.edu.cn (H.Z.).

Notes

The authors declare no competing financial interest.

ACKNOWLEDGMENTS

We thank the National Basic Research Program of China (Grant No. 2011CB605700) and NSFC (Grants No. 20874019, 20990231, and 21104010) for financial support. The computation was made possible by the facilities of SHARCNET (www.sharcnet.ca).

REFERENCES

(1) Bagatolli, L.; Kumar, P. B. S. *Soft Matter* **2009**, *5*, 3234−3248.
(2) Bagatolli, L. A.; Gratton, E. *Biophys. J.* **2000**, *78*, 290−305.
(3) Baumgart, T.; Hess, S. T.; Webb, W. W. *Nature* **2003**, *425*, 821−824.
(4) Li, L.; Liang, X. Y.; Lin, M. Y.; Qiu, F.; Yang, Y. L. *J. Am. Chem. Soc.* **2005**, *127*, 17996−17997.
(5) Yanagisawa, M.; Imai, M.; Taniguchi, T. *Phys. Rev. Lett.* **2008**, *100*, 148102.
(6) Lipowsky, R. *J. Phys. II* **1992**, *2*, 1825−1840.
(7) Taniguchi, T. *Phys. Rev. Lett.* **1996**, *76*, 4444−4447.
(8) Gozdz, W. T.; Gompper, G. *Europhys. Lett.* **2001**, *55*, 587−593.
(9) Kumar, P. B. S.; Gompper, G.; Lipowsky, R. *Phys. Rev. Lett.* **2001**, *86*, 3911−3914.
(10) Kohyama, T.; Kroll, D. M.; Gompper, G. *Phys. Rev. E* **2003**, *68*, 061905.
(11) Li, J. F.; Zhang, H. D.; Tang, P.; Qiu, F.; Yang, Y. L. *Macromol. Theory Simul.* **2006**, *15*, 432−439.
(12) Hong, B. B.; Qiu, F.; Zhang, H. D.; Yang, Y. L. *J. Phys. Chem. B* **2007**, *111*, 5837−5849.
(13) Funkhouser, C. M.; Solis, F. J.; Thornton, K. *Soft Matter* **2011**, *6*, 3462−3466.
(14) Julicher, F.; Lipowsky, R. *Phys. Rev. Lett.* **1993**, *70*, 2964−2967.
(15) Kawakatsu, T.; Andelman, D.; Kawasaki, K.; Taniguchi, T. *J. Phys. II* **1993**, *3*, 971−997.
(16) Gutlederer, E.; Gruhn, T.; Lipowsky, R. *Soft Matter* **2009**, *5*, 3303−3311.
(17) Zheng, C.; Liu, P.; Li, J.; Zhang, Y. W. *Langmuir* **2010**, *26*, 12659−12666.
(18) Hu, J. L.; Weikl, T.; Lipowsky, R. *Soft Matter* **2011**, *7*, 6092−6102.
(19) Chen, C. M.; Higgs, P. G.; MacKintosh, F. C. *Phys. Rev. Lett.* **1997**, *79*, 1579−1582.
(20) Alberts, B.; Wilson, J. H.; Hunt, T. *Molecular biology of the cell*, 5th ed.; Garland Science: New York, 2008.
(21) Svetina, S. *ChemPhysChem* **2009**, *10*, 2769−2776.
(22) Lipowsky, R.; Sackmann, E. *Structure and Dynamics of Membranes*; Elsevier: Amsterdam, The Netherlands, 1995.
(23) Brakke, K. A. *Exp. Math.* **1992**, *1*, 141−165.
(24) Devenyi, G. A.; Li, J. F.; Hughes, R. A.; Shi, A. C.; Mascher, P.; Preston, J. S. *Nano Lett.* **2009**, *9*, 4258−4263.
(25) Jones, R. A. L.; Richards, R. W. *Polymers at Surfaces and Interfaces*, 1st ed.; Cambridge University Press: Cambridge, U.K., 1999.
(26) Dyn, N.; Levin, D.; Gregory, J. A. *ACM Trans. Graphics* **1990**, *9*, 160−169.
(27) Muller, M.; Smirnova, Y. G.; Marelli, G.; Furhrmans, M.; Shi, A. C. *Phys. Rev. Lett.* **2012**, *108*, 228103.
(28) Helfrich, W. *Z. Naturforsch.* **1973**, *28C*, 693−703.
(29) Li, J. F.; Fan, J.; Zhang, H. D.; Qiu, F.; Tang, P.; Yang, Y. L. *Eur. Phys. J. E* **2006**, *20*, 449−457.